Multiyear Hybrid Prediction of Atlantic Tropical Cyclone Activity and the Predictability Sources

CHUAN-CHIEH CHANG AND ZHUO WANG

Department of Atmospheric Sciences, University of Illinois at Urbana–Champaign, Urbana, Illinois

(Manuscript received 2 July 2019, in final form 12 December 2019)

ABSTRACT

A hybrid statistical–dynamical model is developed to predict multiyear variability of Atlantic tropical cyclone (TC) activity. A Poisson model takes sea surface temperature (SST) averaged over the Atlantic main development region (MDR) and the Atlantic subpolar gyre region (SPG) from the initialized CESM prediction as predictors, and skillfully predicts the basinwide TC frequency, accumulated cyclone energy (ACE), landfalling TC frequency, and hurricane and major hurricane days. Further analysis shows that the SPG SST is a more important source of predictability than the MDR SST for multiyear Atlantic TC activity. The comparison between the uninitialized and initialized CESM predictions suggests that the SPG SST is better predicted by the initialized CESM owing to the better prediction of Atlantic meridional overturning circulation, which contributes to the overall more skillful TC predictions. On the other hand, the skillful prediction of the basinwide TC frequency by the uninitialized CESM suggests the role of external forcing in the variability of Atlantic TC activity. The dependence of the hybrid prediction skills on the dynamic model ensemble size is also explored, and an ensemble size of ~20 is suggested as optimal. Further analysis shows that the SPG SST is associated with the variability of vertical wind shear and precipitable water over the tropical Atlantic even when the influence of the MDR SST is controlled. The spatial patterns of vertical wind shear and precipitable water suggest a strong modulation of ACE and hurricane frequency but a relatively weak influence on the basinwide TC frequency. The physical mechanisms between the SPG SST and Atlantic TC activity are discussed.

1. Introduction

Interannual or multiyear tropical cyclone (TC) prediction has been less studied compared to seasonal TC prediction despite the apparent socioeconomic value of skillful TC prediction on this longer time scale (Caron et al. 2018). Tropical sea surface temperature (SST) has been regarded as an essential predictability source for seasonal TC activity (e.g., Chen and Lin 2011, 2013; Klotzbach 2007; Vecchi et al. 2011, 2014), although TC activity may be modulated by extratropical processes (Chang and Wang 2018; Zhang et al. 2016, 2017; Zhang and Wang 2019; G. Zhang et al. 2019). Particularly, the relative SST over the Atlantic main development region (MDR; 10°–20°N, 20°–80°W; Goldenberg and Shapiro 1996), with respect to the global tropical mean, plays an important role in regulating Atlantic TC activity and tropospheric variability (e.g., Caron et al. 2014; Swanson 2008; Vecchi and Soden 2007; Vecchi et al. 2011, 2013; Zhao et al. 2010). The physical framework of relative MDR SST is mainly built upon thermodynamic consideration. The tropospheric warming follows the tropical-mean SST under the weak temperature gradient approximation (Sobel and Bretherton 2000; Sobel et al. 2002), while the moist static energy in the boundary layer is strongly modulated by the local SST (Raymond 1995; Zeng et al. 2000). If the MDR SST warms more than the tropical mean, the destabilization of troposphere favors convection and leads to an increase in Atlantic TC activity (Gualdi et al. 2008; Ramsay and Sobel 2011; Sugi et al. 2012; Vecchi and Soden 2007).

In contrast to seasonal prediction, the sources of predictability on the multiyear time scale are less well studied. While the pioneering studies by Smith et al. (2010) and Dunstone et al. (2011) emphasized the importance of the Atlantic subpolar gyre (SPG) SST in multiyear prediction

Supplemental information related to this paper is available at the Journals Online website: https://doi.org/10.1175/JCLI-D-19-0475.s1.

Corresponding author: Zhuo Wang, zhuowang@illinois.edu

DOI: 10.1175/JCLI-D-19-0475.1

of Atlantic hurricane frequency, Vecchi et al. (2013) and Caron et al. (2014) skillfully predicted Atlantic hurricane frequency using the Atlantic MDR SST and the tropical-mean SST. The relative importance of tropical SST and extratropical SST to multiyear Atlantic TC prediction is not clear.

The Atlantic SPG is the region where the Atlantic multidecadal oscillation (AMO; Zhang and Delworth 2006) or Atlantic multidecadal variability (Knight et al. 2006) has the largest low-frequency SST variance. The AMO modulates several large-scale environmental parameters closely related to TC activity, including tropical SST, sea surface pressure (SLP), vertical wind shear (VWS), tropical precipitation, low-level vorticity, and low-tropospheric convergence on decadal to multidecadal time scales (Caron et al. 2015a; Goldenberg et al. 2001; Knight et al. 2006; Ruprich-Robert et al. 2017; Vimont and Kossin 2007; Zhang and Delworth 2006). In the conventional view, the AMO is tied to the Atlantic meridional overturning circulation (AMOC) and is regarded as a natural mode of climate variability (Kim et al. 2018; R. Zhang et al. 2019). Some recent studies suggested that the AMO is driven by atmospheric noises, particularly the North Atlantic Oscillation, and that ocean dynamics are not an indispensable component of the AMO (Clement et al. 2015; Cane et al. 2017). It was also suggested that the AMO may be driven by external radiative forcing, such as volcanic aerosols, changes in solar irradiance, and greenhouse gases (e.g., Booth et al. 2012; Otterå et al. 2010; Otto-Bliesner et al. 2016). Overall, the physical mechanisms of the AMO have been a topic of active debate. This raises a question about the role of internal variability and external forcing in Atlantic TC variability and prediction on multiyear to decadal time scales.

With improved numerical models and increasingly available computing resources, seasonal prediction of TC activity using high-resolution numerical models has been attempted in recent years (Chen and Lin 2011, 2013; Manganello et al. 2016; Murakami et al. 2015). TCs can be directly tracked in high-resolution numerical model simulations, and it was shown that high model resolution can improve the mean TC frequency as well as the spatial distributions of TC genesis and tracks (Manganello et al. 2012, 2016). High-resolution numerical model prediction, however, may not be computationally feasible for multiyear TC prediction. In addition, dynamical models that can skillfully predict the SST and the large-scale circulation anomalies may still have difficulty realistically representing TC activity (Walsh et al. 2010). Hybrid prediction, which employs predictors derived from coarse-resolution dynamical model predictions, has proven skillful in predicting the Atlantic hurricane frequency on multiyear time scales (Caron et al. 2014, 2018; Vecchi et al. 2013). Previous studies have employed different predictors, such as the MDR SST or the relative MDR SST (Caron et al. 2014; Vecchi et al. 2013) and SLP over the tropical and extratropical North Atlantic (Caron et al. 2015b), and the skill of some hybrid predictions is comparable to that of dynamical predictions (Caron et al. 2018).

In this study, we develop a hybrid prediction framework using a newly available decadal prediction dataset and will address the following questions:

- What is the relative importance of different predictors in multiyear Atlantic TC prediction?
- What is the optimal ensemble size for multiyear hybrid TC prediction?
- Does dynamic initialization of the ocean improve the prediction skill?
- What are the physical links between the different predictability sources and Atlantic TC activity?

The data and methodology are described in section 2. The first three questions are addressed using a hybrid prediction framework in section 3; the last question is explored in section 4. Concluding remarks and discussion are presented in section 5.

2. Data and methodology

a. *Global climate model hindcasts and observational datasets*

The hybrid statistical–dynamical models are built on SST indices derived from initialized and uninitialized climate model predictions. The initialized hindcasts are taken from the Community Earth System Model decadal prediction dataset (CESM-DP; Yeager et al. 2018). The atmospheric component of the CESM-DP, the Community Atmosphere Model, version 5 (CAM5; Hurrell et al. 2013), is configurated at a horizontal resolution of 0.94° × 1.25° (latitude × longitude) with 30 vertical levels. The ocean model is the Parallel Ocean Program, version 2 (POP2; Danabasoglu et al. 2012), which is configured at a nominal 1° horizontal resolution on the displaced pole grid and has 60 vertical levels. The experiment includes 40 ensemble members, which are initialized on 1 November every year during 1954–2015 (62 yr) and are integrated for 122 months (~10 yr). Initial conditions for atmospheric and land models in the CESM-DP are obtained from the restart files at the corresponding historical moments from the CESM Large Ensemble (CESM-LE) simulations (described below). The ocean and sea ice initial conditions in the CESM-DP are derived from an updated forced ocean–sea ice simulation (FOSI; Yeager et al. 2018), in which the ocean and sea ice models are driven by the observed time-varying atmospheric states and radiative fluxes. Although no observation is directly assimilated

into the ocean and sea ice models, the FOSI shows a good agreement with the late-twentieth-century ocean observations in the North Atlantic (Yeager et al. 2012; Yeager and Danabasoglu 2014).

The CESM-LE (Kay et al. 2015) has 40 ensemble members, and each member is continuously integrated from 1920 to 2100. The ensemble members are initialized by perturbing the atmospheric initial condition at the round-off level. The CESM-LE shares the same radiative forcing as the CESM-DP experiment. The historical radiative forcing, including the influence from volcanic aerosols, is used to drive the CESM hindcasts for 1920–2005, and the projected radiative forcing of RCP8.5 is used after 2005. In short, the CESM-DP and CESM-LE are based on the same model version (CESM 1.1), have the same model configuration, and share the same historical radiative forcing, and only differ in the initialization of the ocean and sea ice components. The comparison between the two experiments thus helps identify the value of ocean initialization for multiyear prediction. The 40-member ensemble-mean SST from each experiment (CESM-DP or CESM-LE) is used to derive predictors for the hybrid predictions.

Tropical cyclone observations from the HURDAT2 (Landsea and Franklin 2013) are used to develop and evaluate the hybrid predictions; SST data from the Extended Reconstructed Sea Surface Temperature, version 5 (ERSSTv5; Huang et al. 2017), are used as the truth to evaluate the CESM SST predictions; and the NCEP–NCAR Reanalysis 1 (Kalnay et al. 1996) is used to investigate the physical processes linking SST predictors to Atlantic TC activity. We focus on the Atlantic hurricane season, June to November (JJASON), and adopt a 5-yr time window to facilitate the comparison with previous studies (e.g., Caron et al. 2014, 2015b, 2018; Vecchi et al. 2013). The 5-yr running means of JJASON seasonal means of various variables (including SST indices, TC indices, and environmental fields) are examined if not specified otherwise.

b. Predictor selections

To select effective SST predictors, the Pearson correlation coefficient between the observed Atlantic TC frequency and observed SST at every grid point is calculated (Fig. 1a). Strong positive correlations are found over the tropical Atlantic MDR, the subpolar North Atlantic, and the Pacific. In particular, the SST correlation pattern over the Pacific resembles the negative phase of the Pacific decadal oscillation (PDO; Zhang et al. 1997), and the SST pattern over the Atlantic resembles the positive phase of the AMO. This suggests that remote SST anomalies, from either the extratropical Atlantic or the Pacific, may modulate Atlantic TC activity in addition to the local SST anomalies over the tropical Atlantic (e.g., Li et al. 2015).

The CESM-DP broadly reproduces the observed correlation patterns over the North Atlantic and the Pacific (Fig. 1b), including the strong positive correlations over the tropical Atlantic, the Atlantic SPG, and the western North Pacific. However, the CESM-DP does not capture the significant negative correlation over the tropical eastern Pacific, resulting from the deficiency of the model in predicting the tropical Pacific SST anomalies (Yeager et al. 2018). Further investigation suggests that the model fails to reproduce the PDO despite the moderate prediction skill of SST over the extratropical North Pacific (not shown). Additionally, Fig. 1b shows basinwide positive correlations, instead of a tripole pattern (Czaja and Marshall 2001), over the North Atlantic.

Various possible SST predictors—the MDR SST, SPG SST (50°–60°N, 10°–50°W; Caron et al. 2015b), Niño-3.4 SST, an SST index representing the western North Pacific (30°–40°N, 135°E–180°), and the tropical-mean SST (between 30°S and 30°N)—are tested (see Table S1 in the online supplemental material), and the combination of the MDR and SPG SST indices produces the most skillful prediction. Inclusion of the Niño-3.4 SST or the western North Pacific SST does not help appreciably increase the prediction skills. Compared to the other sets of SST predictors, the relative MDR SST (predictor set 2) exhibits lower prediction skill, especially for the accumulated cyclone energy prediction across all forecasting lead times (Table S1). These results, however, are likely model dependent, and can probably be attributed to the poor skill of the CESM-DP in predicting ENSO (Yeager et al. 2018) and the tropical-mean SST.

Since the MDR and SPG SST indices are not independent of each other, we assess the impact of collinearity using the variance inflation factor (VIF; Davis et al. 1986). The VIF values of the two SST predictors (2.75, 4.71, and 2.15 for ERSSTv5, CESM-DP, and CESM-LE, respectively) are lower than the VIF cutoff value of 10, which is commonly used to drop off a predictor (e.g., Villarini et al. 2012). Both predictors are thus employed in the hybrid model.

c. Statistical component of the hybrid prediction

The statistical emulator is formulated as a Poisson regression model with two predictors: MDR SST and SPG SST. The regression equation can be written as

$$\lambda = \exp(a_0 + a_1 \mathrm{SST}_{\mathrm{MDR}} + a_2 \mathrm{SST}_{\mathrm{SPG}}),$$

where $\mathrm{SST}_{\mathrm{MDR}}$ and $\mathrm{SST}_{\mathrm{SPG}}$ are the MDR and SPG SST anomalies relative to the model climatology at the corresponding lead times (the time periods associated with different forecasting lead times are shown in the online supplemental material); λ represents different TC

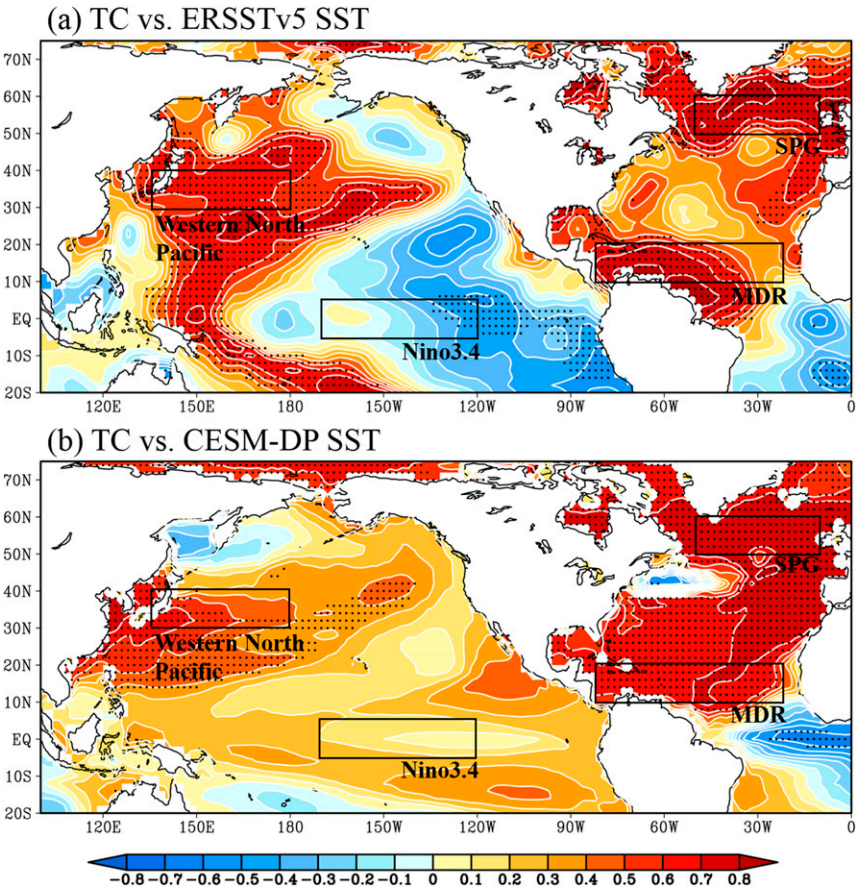

FIG. 1. (a) Pearson correlation coefficients between the observed 5-yr-mean global SST and the Atlantic TC frequency from HURDAT2 over 1955–2016. (b) As in (a), but the global SST is taken from the first 5 years of the CESM-DP. Black dots indicate correlations exceeding the 95% confidence level based on the Student's *t* test. The black boxes depict the regions used to define the MDR, SPG, western North Pacific, and Niño-3.4 SST indices. Note that the significance level is determined based on the effective sample size, which varies from grid point to grid point (see section 2d).

indices, including the basinwide TC frequency, accumulated cyclone energy (ACE), landfalling TC frequency, landfalling hurricane frequency, hurricane days, and major hurricane days. A TC making landfall anywhere in the U.S. coastline, the Mexico coastline, or the Caribbean islands during its lifetime is regarded as a landfalling TC, and a category 3–5 hurricane is defined as a major hurricane. Different from many previous studies, the predictors and predictands are linearly detrended before fitting the Poisson regression model. We deem detrending a necessary step because noticeable linear trends exist in the predictors and the predictands and would artificially inflate the prediction skill.

d. *Assessment of prediction skill and statistical significance*

Prediction skill is assessed primarily by the Pearson correlation between the predicted and observed time series of TC indices using a leave-5-years-out cross-validation method (Wilks 2006). For example, to predict the 5-yr-mean TC frequency centered on 2009, the 5 years 2007–11 are excluded from the training data, and the 5-yr running means of SST predictors and the observed TC frequency during 1955 to 2006 (i.e., 5-yr running means from 1955–59 to 2002–06) are used to fit the Poisson regression model via the maximum likelihood method (McCullagh and Nelder 1989). This is repeated for every 5-yr running mean and produces a time series of the predictand.

Strong autocorrelations exist in the predictor and predictand time series, which reduces the degree of freedom of the data. The effective degree of freedom N^* is estimated following Chelton (1984):

$$N^* = \frac{N}{1 + 2\sum_{j=1}^{N/4} \rho_{xx}(j)\rho_{yy}(j)},$$

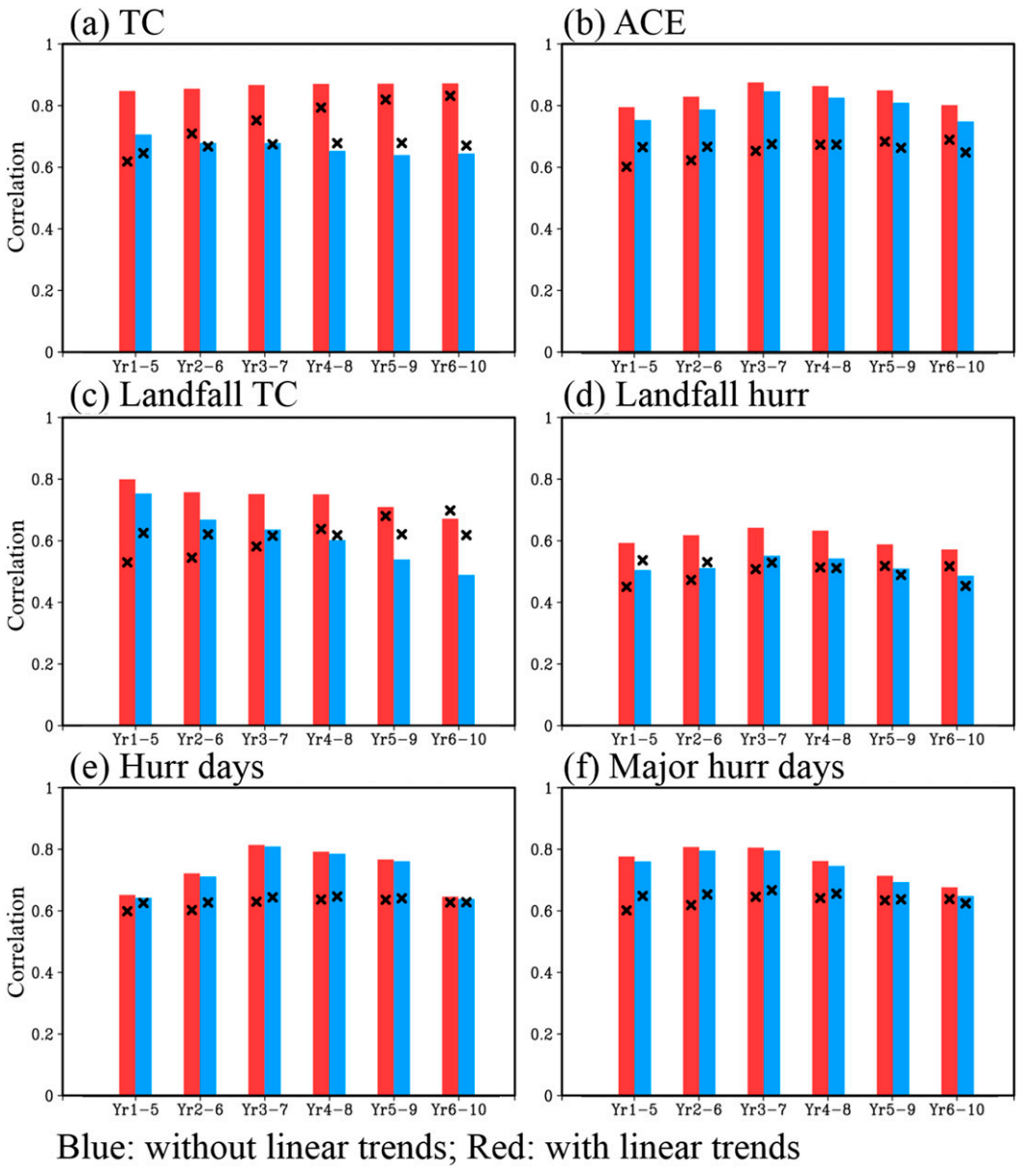

FIG. 2. Prediction skills of (a) basinwide TC frequency, (b) ACE, (c) landfalling TC frequency, (d) landfalling hurricane frequency, (e) hurricane days, and (f) major hurricane days at different forecast lead times. The × marks indicate the 95% confidence levels based on adjusted degrees of freedom. Blue bars represent the skills when both the SPG and MDR SST are used as the predictors. The red bars show the prediction skills when the observed linear trends of TC activity are added back.

where $\rho_{xx}(j)$ and $\rho_{yy}(j)$ are the autocorrelations of time series x, y at lag j, respectively, and N is the length of the time series. Since the autocorrelation of a field variable varies from grid point to grid point, the effective degree of freedom also has spatial variability. Although there are more than 50 years of data, the effective degree of freedom of the 5-yr-mean time series is between 8 and 10. The significance of the Pearson correlation is determined based on the effective degree of freedom using the Student's t test. Root-mean-square error (RMSE) is also examined for some predictions, but prediction skill is referred to the Pearson correlation if not specified otherwise.

3. Hybrid prediction of Atlantic TC activity

a. Retrospective forecasts

Figure 2 shows the prediction skill of the hybrid model using the MDR SST and the SPG SST as predictors. The ACE, landfalling TC frequency, landfalling hurricane frequency, hurricane days, and major hurricane days are

examined in addition to the basinwide TC frequency. The correlations exceed the 95% confidence level for ACE, hurricane days, and major hurricane days across all forecast lead times, and the model is skillful in predicting the basinwide and landfalling TC frequencies from Yr 1–5 to Yr 3–7. The hybrid predictions of TC frequency and ACE are also compared with the persistence forecasts, in which the 5-yr-mean persistence is defined as the observed average over the 5 years preceding the CESM-DP initialization. For example, the persistence forecast of ACE for Yr 1–5 prediction centered on 1995 (i.e., model initialized in November 1992) is the observed ACE averaged from 1988 to 1992. The hybrid model outperforms the persistence forecasts at all forecast lead times (Table S1 in the online supplemental material). We also tried adding the observed linear trends to the TC indices, and it brings the prediction skill higher except for hurricane days and major hurricane days, which do not have a strong linear trend.

In addition to the Pearson correlation, the skill of hybrid predictions is also evaluated using RMSE (Fig. S2). The RMSEs of TC frequency, landfalling TC frequency, and landfalling hurricane frequency are around 1.2, 0.9, and 0.6, respectively; the RMSEs of hurricane days and major hurricane days are 4–6 and ~2, respectively; and the RMSE of ACE is less than 20. Overall, our results suggest that skillful prediction of multiyear variability of the basinwide and landfalling TC activity is feasible.

To compare the relative contribution of the MDR and SPG predictors, the prediction skill of multiyear TC activity is shown in Fig. 3, where the MDR or SPG SST is used as the sole predictor without adding the linear trends. The prediction skill is consistently higher for all the TC indices across all forecast lead times when the SPG SST is used as the sole predictor than when the MDR SST is used as the sole predictor, except for the basinwide TC frequency and landfalling TC frequency at Yr 1–5. In fact, using the MDR SST alone fails to skillfully predict ACE, landfalling hurricane frequency, hurricane days, or major hurricane days at any forecast lead times. This suggests that the SPG SST is a more important predictability source for multiyear Atlantic TC activity than the MDR SST in the CESM-DP. These results do not necessarily contradict the previous studies emphasizing the role of the MDR SST (Vecchi et al. 2013; Caron et al. 2014), because using the MDR SST alone can skillfully predict the basinwide TC frequency and landfalling TC frequency at Yr 1–5 and Yr 2–6. Additionally, the relative importance of the two predictors in the hybrid predictions may be model dependent. The role of the SPG SST in modulating the large-scale circulation is discussed in the section 4.

b. *The skill dependence on ensemble size*

Ensemble prediction has become a common practice in recent years. Model uncertainties may arise from the uncertainties of the initial conditions and uncertainties of the model physics. The ensemble mean helps reduce uncertainties and increase the signal-to-noise ratio. On the other hand, a larger ensemble size requires more computing resources. It is thus helpful to investigate the optimal number of ensemble members for skillful prediction given limited computing resources. The Pearson correlation and RMSE as a function of the ensemble size (Fig. 4) are computed using the bootstrap resampling. For an ensemble size N, the 5-yr-averaged ensemble-mean MDR and SPG SSTs are calculated from N members randomly chosen from the pool of 40 CESM-DP members. This is done independently for each year during 1954–2006, and the correlations and RMSEs of TC frequency and ACE are then calculated. The distributions of Pearson correlation and RMSE for the ensemble size of N are obtained by repeating this procedure 1000 times. This can be done for different ensemble sizes between 1 and 39 (note that the ensemble members are chosen independently for each year). The median, 95th and 5th percentiles of the correlation, and RMSE values are shown in Fig. 4. The correlation coefficients increase sharply when the ensemble size is increased from 1 to 5 and saturates when the ensemble size is around 20, consistent with the previous studies based on high-resolution numerical model simulations (Manganello et al. 2016; Mei et al. 2019) or for operational hurricane forecasts (Gall et al. 2013). The RMSE of TC frequency decreases sharply from 1 to 5 and starts to level off for the ensemble size around 20. The RMSE of ACE, however, decreases more gradually and does not converge even for the ensemble size 40.

c. *Initialized and uninitialized prediction*

The role of ocean initialization is explored by comparing the skill of the hybrid prediction using the SST predictors from the CESM-DP to that using the SST predictors from the CESM-LE (Fig. 5). The Poisson model [Eq. (1)] is trained for the SST predictors from the CESM-DP and CESM-LE separately. The initialized (CESM-DP) and uninitialized (CESM-LE) predictions show similar skills in predicting the basinwide TC frequency, landfalling TC, and hurricane frequencies for short lead times, but the skill of the uninitialized prediction deteriorates quickly for longer lead times. The uninitialized predictions of ACE, hurricane days, and major hurricane days show no skill at all. The initialized prediction outperforms the uninitialized prediction except for the basinwide and landfalling TC

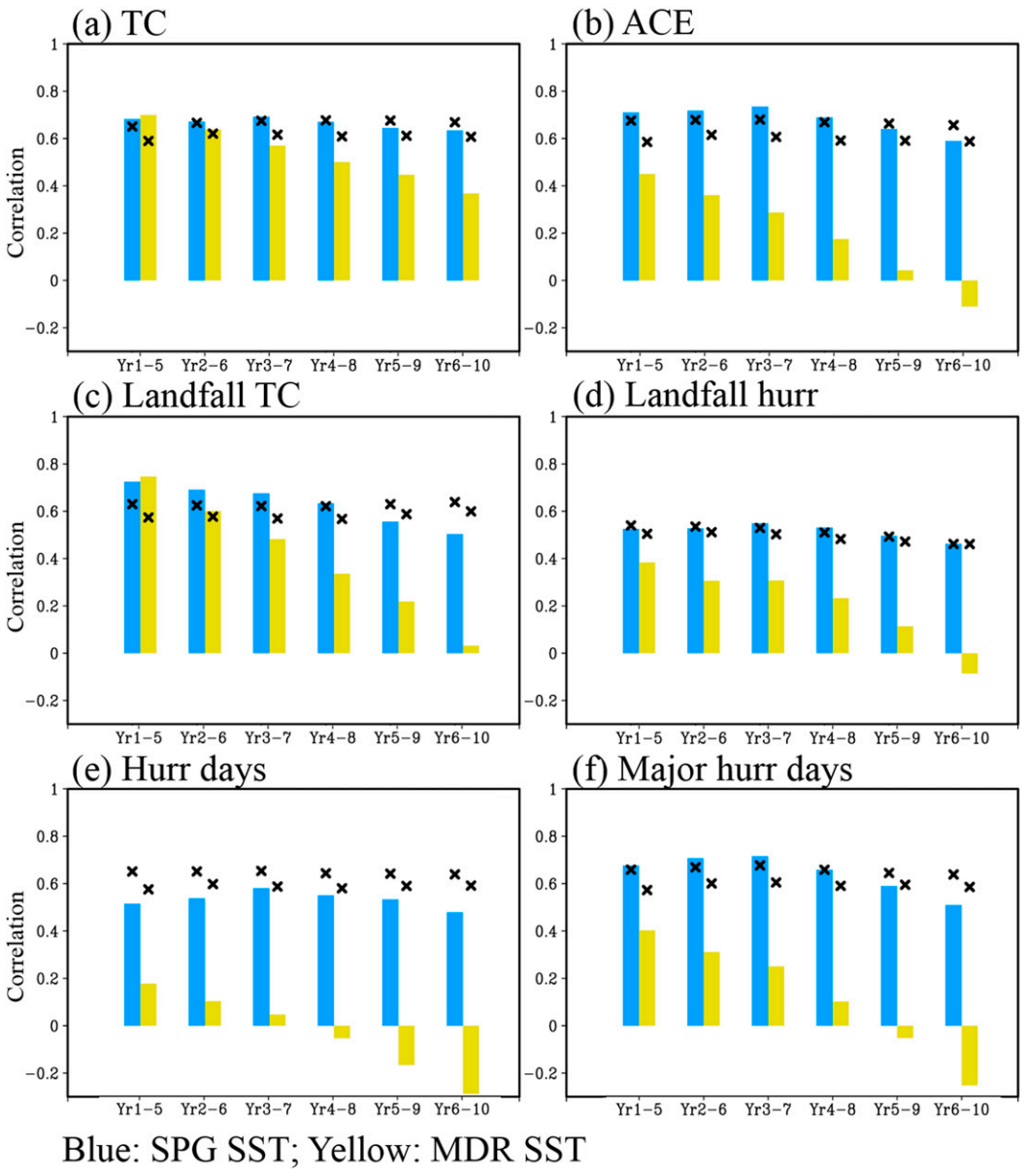

FIG. 3. Prediction skills of various TC indices at different forecast lead times. The × marks indicate the 95% confidence levels based on adjusted degrees of freedom. The blue and yellow bars represent the skills when the SPG and MDR SST are used as the only predictor, respectively.

frequencies at short lead times, and the prediction skills assessed by RMSE show consistent findings (Fig. S2). The increase in prediction skill via model initialization is in line with some previous studies (Smith et al. 2010; Vecchi et al. 2013). These results lead to two questions: What is the source of predictability in the uninitialized CESM-LE prediction? Why does the ocean initialization contribute to the ACE prediction but not much to the TC frequency prediction?

To answer the first question, we evaluate the prediction of the two SST indices against the ERSSTv5. The CESM-DP and CESM-LE show a similar skill in predicting the MDR SST (Fig. 6a), although both predictions have 1–2-K cold biases in MDR SST (not shown), a common issue for CMIP5 climate models (Zhang and Zhao 2015). In contrast, the CESM-DP is much more skillful than the CESM-LE in predicting the SPG SST (Fig. 6b). In fact, the CESM-LE shows no skill in predicting the SPG SST.

The MDR SST and SPG SST can be regarded as the tropical and extratropical components of the AMO, respectively. The recent study by Delworth et al. (2017)

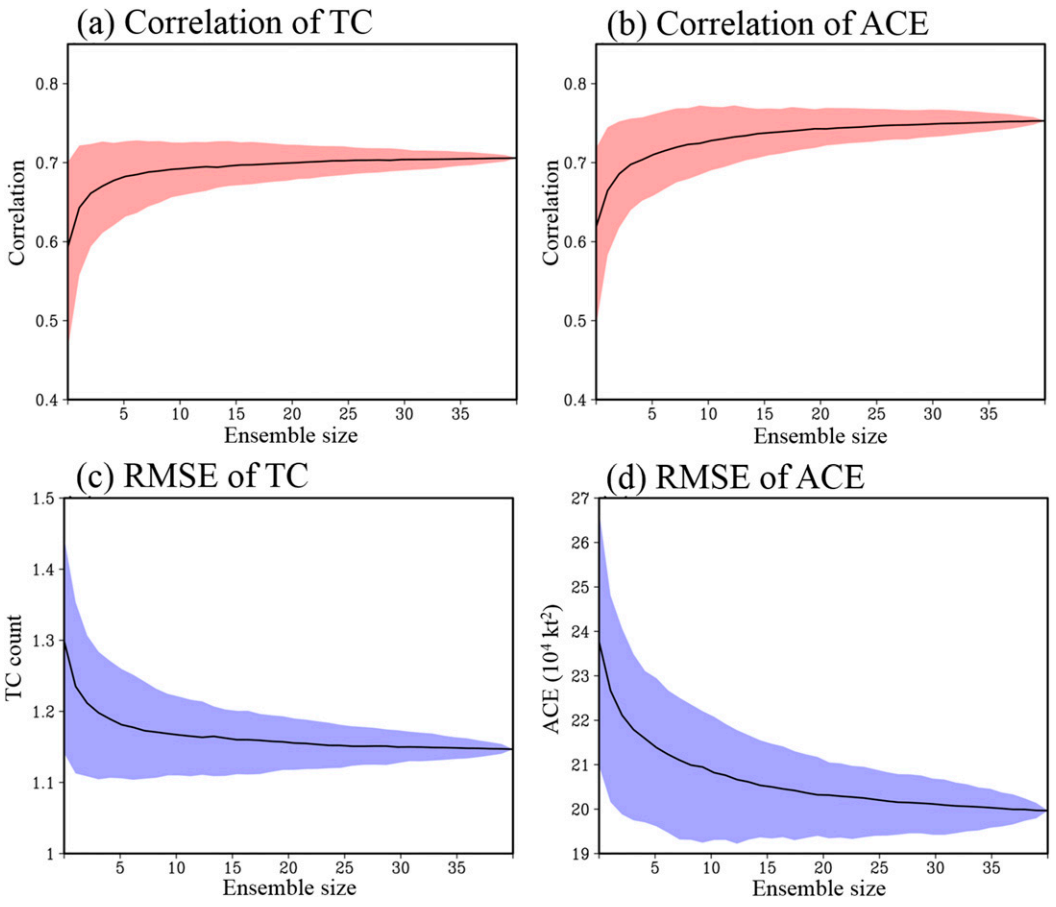

FIG. 4. (top) The prediction skill of (a) the basinwide TC frequency and (b) ACE as a function of the dynamical model ensemble size. (bottom) The RMSEs of (c) the basinwide TC frequency and (d) ACE as a function of the dynamical model ensemble size, respectively. Shading represents the 5%–95% uncertainty range. SST predictors are taken from the first 5 years of the CESM-DP.

emphasized the role of ocean dynamics in generating extratropical Atlantic SSTA as a delayed response to the Atlantic meridional overturning circulation (AMOC). The CESM-DP underestimates the strengths of AMOC and northward heat transport at 50°N, but skillfully captures their variabilities on the multiyear to interdecadal time scales, while the CESM-LE shows no skill (Fig. 7). In contrast to the extratropical Atlantic SST, the radiative forcing associated with anthropogenic or natural aerosols and dust emission (Booth et al. 2012; Evan et al. 2008, 2009) was suggested to play an important role in the variability of the tropical Atlantic SST. Recall that the CESM-DP and CESM-LE share the same radiative forcing, which explains the skillful prediction of the MDR SST by both experiments, while the poor prediction of the SPG SST by the CESM-LE is consistent with the important role of ocean dynamics in the variability of extratropical Atlantic SST on the multiyear time scale. The comparison between the hybrid predictions based on the CESM-LE and CESM-DP thus also implies the role of external forcing in the variability of Atlantic basinwide TC frequency and landfalling TC frequency.

The finding that the initialized prediction has higher skill than uninitialized prediction in predicting ACE but has similar skills in predicting basinwide TC frequency is consistent with Fig. 3, which shows that the SPG SST is more skillful in predicting ACE than the MDR SST but the two SST predictors have comparable skill in predicting the basinwide TC frequency. This issue is further examined in the next section.

4. The physical mechanisms behind the predictability sources

a. Implications for different large-scale variables

The importance of the relative MDR SST in modulating the large-scale circulation over the North Atlantic from the seasonal to multiyear time scales has been investigated by some previous studies (e.g., Bell and

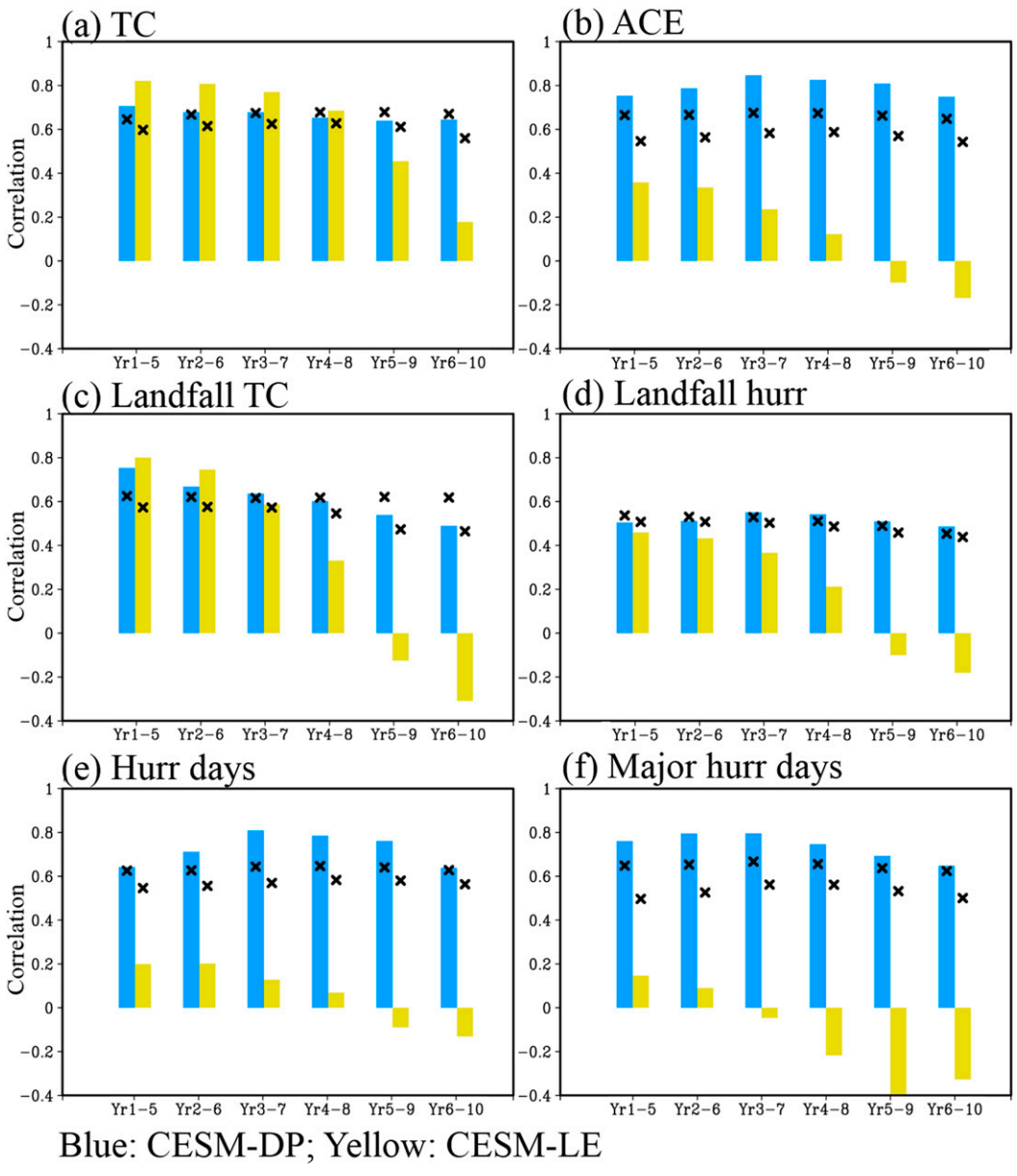

FIG. 5. Prediction skills of various TC indices at different forecast lead times. The × marks indicate the 95% confidence levels based on adjusted degrees of freedom. The blue and yellow bars represent the skills based on the CESM-DP and the CESM-LE, respectively.

Chelliah 2006; Camargo et al. 2007; Latif et al. 2007; Swanson 2008; Vecchi and Soden 2007). In comparison, the SPG SST has been less well studied. The more skillful predictions of some TC indices using the SPG SST suggest that the SPG SST might independently modulate the atmospheric circulation over the tropical Atlantic. Since the SPG SST and the MDR SST are not independent of each other, here we calculate the partial correlations to disentangle their relative impacts on environmental variables. The total precipitable water (TPW) and VWS (defined as the magnitude of the vector wind difference between 200 and 850 hPa) during the Atlantic TC season (June–November) are examined. The seasonal-mean fields are derived from the NCEP–NCAR Reanalysis 1 (Kalnay et al. 1996). All variables are linearly detrended, and a 5-yr running-mean filter is applied between 1955 and 2016. For the partial correlation between the MDR SST and a variable x, the influences of the SPG SST on the MDR SST and x are removed by linear regression, and then the

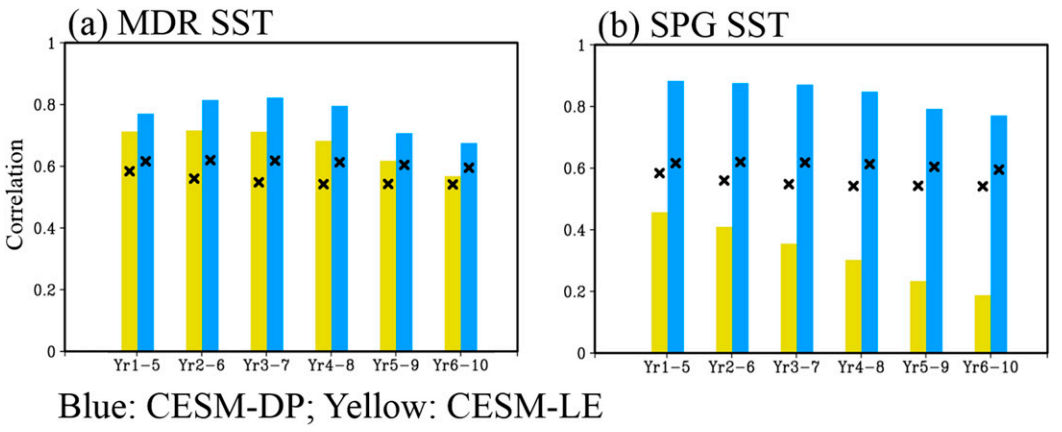

FIG. 6. Prediction skills of (a) MDR SST and (b) SPG SST in the CESM-DP (blue) and the CESM-LE (yellow) at different forecast lead times. The × marks indicate the 95% confidence levels based on adjusted degrees of freedom.

Pearson correlation is calculated between the residuals of the MDR SST and x. A similar calculation is done for the partial correlation between the SPG SST and x by controlling the influences of the MDR SST on the SPG SST and x.

Figure 8 shows that the MDR SST and the SPG SST both impact the TPW and VWS over the tropical and subtropical Atlantic, but the impacts have different spatial patterns. Figure 8a suggests that positive TPW anomalies prevail north of 10°N when the MDR SST is warm, in keeping with the satellite observations (Wentz and Schabel 2000). Consistent with some previous studies (e.g., Sutton and Hodson 2007; Zhang and Wang 2013), the warm anomalies of MDR SST are associated with reduced VWS throughout the MDR and over the southeastern United States (Fig. 8b). The partial correlation is very weak in the subtropical Atlantic. Overall, the correlation patterns suggest that the warm MDR SST favors an increase in the basinwide TC frequency and ACE.

The partial correlations of the SPG SST with the TPW show a patchy pattern, with weak correlations in the subtropical western Atlantic and a small region of significant positive correlations over the east Atlantic (Fig. 8c), which may reflect the relationship between the AMO and West African rainfall (e.g., Diatta and Fink 2014; Martin and Thorncroft 2014) given the strong link between the AMO and SPG SST (e.g., Sutton 2005; Ruprich-Robert et al. 2017). Figure 8d suggests that the warm SPG SST anomalies are associated with reduced VWS over the MDR (Fig. 8d) but enhanced VWS over tropical West Africa, the southeastern United States, and the subtropical Atlantic. The combined TPW and VWS patterns suggest an environment conducive to TC activity over the east Atlantic but a possibly hostile environment over the subtropical western Atlantic. It may affect the chance of TCs to intensify into hurricanes but may not strongly modulate the basinwide TC frequency (Zhang et al. 2017), which explains why the predictions of ACE and hurricane days are more sensitive to the SPG predictor than the prediction of the basinwide TC frequency. In summary, our analyses suggest that SPG SST can significantly influence TPW and VWS independent of the MDR SST forcing.

The impacts of SPG SST on different environmental variables raise the following question: how does the SPG SST modulate the atmospheric circulation over the tropical Atlantic? It may be understood in the framework of the Atlantic regional Hadley circulation (Zhang and Wang 2013). As suggested by several previous studies (e.g., Bellomo et al. 2016; Chiang et al. 2003; Chiang and Bitz 2005; Dunstone et al. 2011; Yuan et al. 2016), the extratropical SST anomalies may modulate the ITCZ through changes in the tropical SST via the wind–evaporation feedback or the cloud–radiation feedback, and a sudden weakening of the AMOC can induce dipolar SST anomalies in the tropical Atlantic and leads to a meridional displacement of ITCZ (Dong and Sutton 2002; Okumura et al. 2009; Zhang and Delworth 2005). The idea may seem consistent with the studies about the impacts of extratropical forcing on the ITCZ in the energy framework (Broccoli et al. 2006; Kang et al. 2008, 2009), but the applicability of the energy framework to the regional Hadley circulation is not clear as one needs to consider the zonal energy transport by the ocean and the atmosphere for the regional energy budget. It is thus instructive to examine the link between the SPG SST and the regional Hadley circulation.

Following Zhang and Wang (2013), we calculate the regional meridional streamfunction over 20°–80°W using the JJASON seasonal-mean irrotational meridional

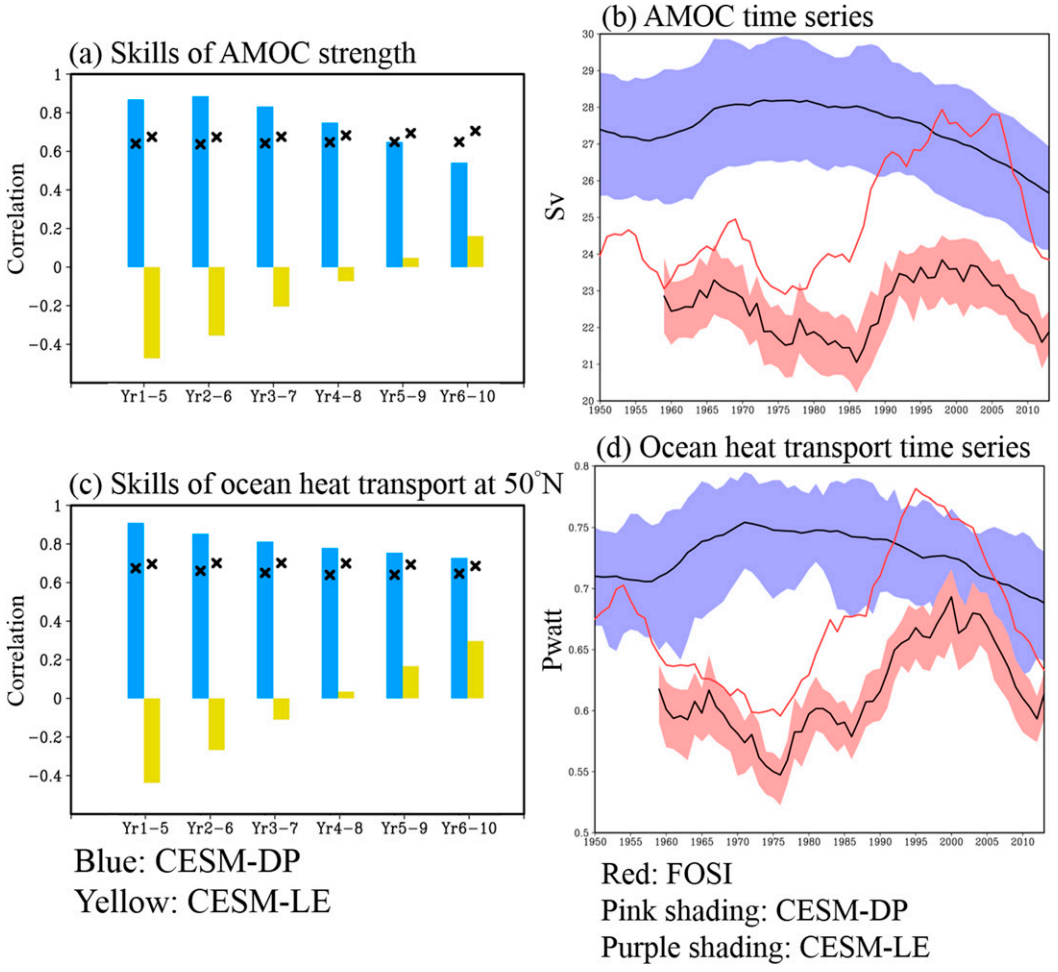

FIG. 7. (a) Forecast skills of the AMOC strength at different lead times in the CESM-DP (blue bars) and the CESM-LE (yellow bars). The × marks indicate the 95% confidence levels based on adjusted degrees of freedom. (b) The 5-yr-mean AMOC strength (Sv; 1 Sv ≡ 10^6 m^3 s^{-1}) time series in the FOSI (red), the CESM-DP at Yr 3–7 (black line with pink shading), and the CESM-LE (black line with purple shading). Shading parts represent the 5th–95th-percentile range of the ensemble members. The forecasts are aligned to the central years of the 5-yr-average periods. (c) As in (a), but for northward ocean heat transport (PW) at 50°N in the North Atlantic. (d) As in (b), but for ocean heat transport at 50°N.

flow component derived from NCEP–NCAR Reanalysis 1 (Figs. 9a,b), along with precipitation (1979–2017) from the Global Precipitation Climatology Project (GPCP) (Figs. 9c,d; Adler et al. 2003). The most prominent cell in the long-term-mean streamfunction is the southern Hadley cell, with the ascending branch located slightly north of the equator and the downward motion between 15° and 30°S. The mean position of regional ITCZ indicated by the precipitation peak agrees well with the ascending branch of the Hadley cells, and weak precipitation around 20°S/N is consistent with the descending motion of the Hadley circulation.

The streamfunction anomalies corresponding to the warmer SPG SST exhibit an interhemispheric dipole pattern, indicating a slight northward displacement of the strengthened southern Hadley cell (Fig. 9a). Although the anomalous precipitation signal associated with variability of SPG SST is relatively weak (Fig. 9c), it is qualitatively in line with the streamfunction anomalies shown in Fig. 9a. Both datasets describe an intensification of the ascending branch of the regional Hadley circulation. The negative streamfunction anomalies between 15° and 30°N (Fig. 9a), along with the increased precipitation around 20°N (Fig. 9c), reveal the reduced subsidence in the subtropics due to the weakening of the northern Hadley cell.

After the removal of possible influence from the MDR SST, the partial linear regressions of streamfunction and

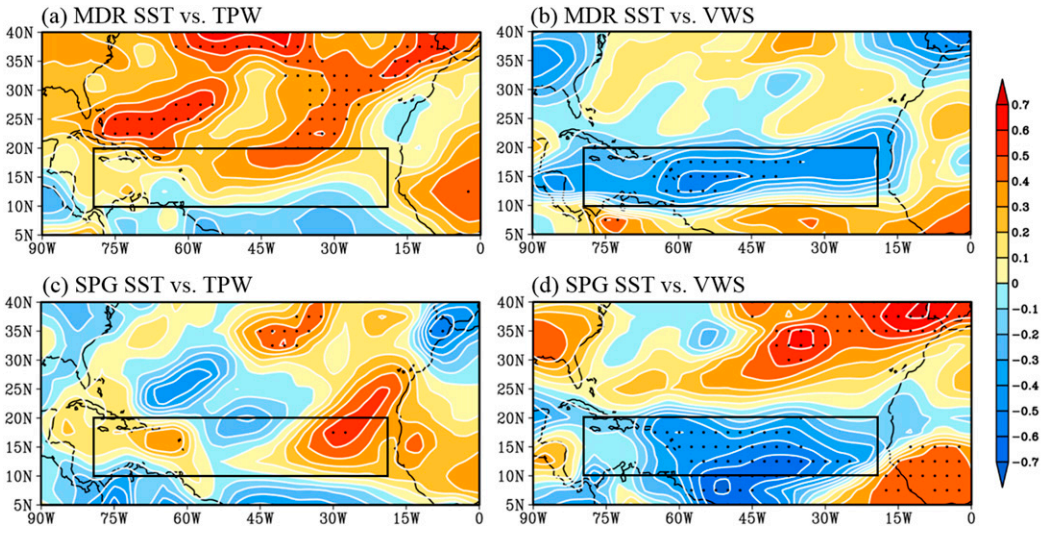

FIG. 8. Partial correlation between the 5-yr-mean SST indices and 5-yr-mean (left) TPW and (right) VWS during 1955–2016. The correlations with (top) the MDR SST and (bottom) the SPG SST. SST indices are derived from the ERSSTv5. Black dots indicate the regions exceeding 95% confidence level based on the Student's *t* test. The black box highlights the Atlantic MDR.

precipitation onto the SPG index (Figs. 9b,d) show similar patterns to Figs. 9a and 9c but with generally weaker magnitudes, and significant anomalies of streamfunction now mainly occur in the upper troposphere, and still indicate the strengthening and slight northward displacement of the southern cell and the weakening of the northern cell. Overall, the strengthening of the ITCZ and the weakening of the subtropical subsidence both favor Atlantic TC activity (Zhang and Wang 2013), but the regional differences between the west and east Atlantic as shown in Fig. 8a cannot be revealed by the zonal-mean circulation.

b. *Possible linkage to the Pacific decadal oscillation and the Atlantic intrabasin SST contrast*

Figure 10 shows the partial correlations between the SPG or MDR SST index and global SSTs. After removing the influence of the MDR SST, the SST pattern associated with the SPG SST over the Pacific resembles the negative phase of the PDO (Zhang et al. 1997). The PDO has been suggested as a response to the AMO through atmospheric teleconnections and oceanic dynamics (Yu et al. 2015; Zhang and Delworth 2007). Observational and modeling studies (McGregor et al. 2014; Sohn et al. 2013) suggested that SST anomalies over the tropical Pacific may modulate the Walker circulation and lead to the variability of the Atlantic Hadley circulation (Chiang 2002), which contributes to the variability of Atlantic TC activity (Zhang and Wang 2013). We note that the PDO is strongly anticorrelated to the 5-yr-mean Atlantic TC frequency ($r = -0.62$), consistent with Li et al. (2015). Additionally, a significant negative correlation is found between the observed PDO and SPG SST indices ($r = -0.56$), indicating that the influence of the Pacific SST is implicitly represented by the SPG SST. It is possible that the regional ITCZ variability associated with changes in the SPG SST involves variations in tropical Atlantic SST and also reflects the teleconnection between the subpolar North Atlantic oceanic variability and the Pacific climate mode on the decadal time scale (Chafik et al. 2016). Another noticeable feature is the east–west dipole pattern over the Atlantic, which can be represented by a dipole index (see the two highlighted regions in Fig. 10b). Further analysis reveals a significant partial correlation between the 5-yr-mean Atlantic TC frequency and the 5-yr-mean dipole SST index ($r = 0.57$) when the influence of the MDR SST is controlled, suggesting another pathway for the SPG SST to affect the tropical Atlantic circulation. The link between the dipole-pattern SSTAs and the tropical Atlantic circulation merits further investigation but is outside the scope of the present study.

5. Summary and discussion

We develop a skillful statistical–dynamical model for multiyear prediction of Atlantic TC activity. The dynamical predictions of SST are based on recently conducted CESM-DP (Yeager et al. 2018). The statistical component of the hybrid model is a Poisson model that takes the Atlantic MDR and SPG SST indices as predictors. The hybrid prediction is evaluated against the

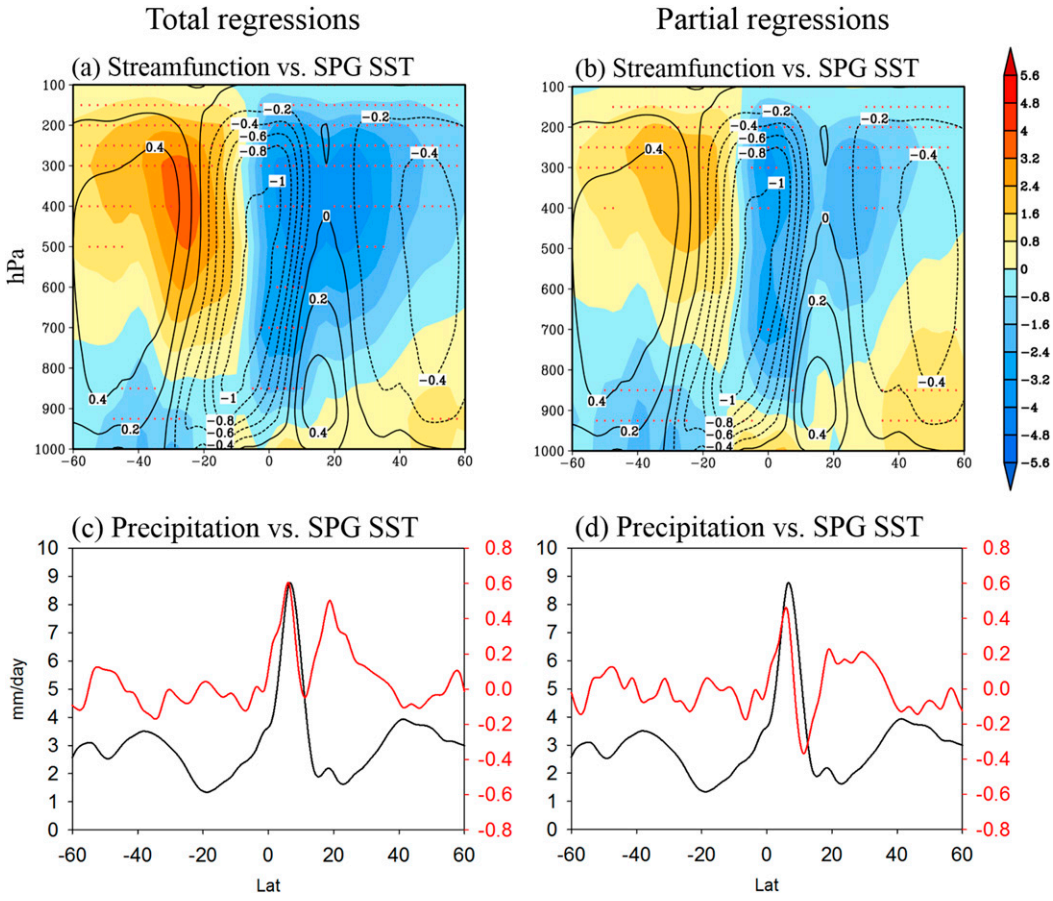

FIG. 9. (a) Long-term JJASON seasonal-mean streamfunction from 1955 to 2016 (contours;10^{11} kg s^{-1}) and streamfunction anomalies (shading; 10^{10} kg s^{-1}) regressed onto one standard deviation (1σ) of the 5-yr-mean detrended SPG SST. Red dots indicate the regressions exceeding the 95% confidence level based on the Student's t test. (b) As in (a), but for streamfunction anomalies partially regressed onto 1σ of the 5-yr-mean detrended SPG SST after the influence of the MDR SST is removed. (c) JJASON-mean precipitation from 1979 to 2017 (black curve with the ordinate on the left) and precipitation anomalies (red curve with the ordinate on the right) regressed onto 1σ of the 5-yr-mean detrended SPG SST. (d) As in (c), but for precipitation anomalies partially regressed onto 1σ of the 5-yr-mean detrended SPG SST after the influence of the MDR SST is removed.

HURDAT2 data using the leave-5-years-out method, and the hybrid model exhibits significant skills for the basinwide TC frequency, ACE, and landfalling TC frequency, as well as hurricane and major hurricane days.

Further investigation reveals that the SPG SST is an important source of predictability, and the predictions based on the SPG SST alone demonstrate higher skill than those based on the MDR SST alone. In addition, the dependence of retrospective forecast skill on the ensemble size is explored. The prediction skill based on the Pearson correlation quickly increases when the ensemble size is increased from 1 to 5 and saturates when the ensemble size is around 20, similar to the dynamic prediction of seasonal TC activity (Manganello et al. 2016; Mei et al. 2019), but the RMSE of ACE does not converge even for the ensemble size of 40.

The impacts of ocean initialization on prediction skill are examined by comparing the hybrid predictions based on the CESM-DP and CESM-LE experiments (Kay et al. 2015), with the latter serving as the uninitialized counterpart to the CESM-DP. Initialization of ocean and sea ice does not strongly affect TC frequency prediction, but significantly increases the prediction skill of ACE, landfalling hurricane frequency, and hurricane and major hurricane days. Further analysis shows that the variability of the AMOC and the SPG SST are skillfully predicted in the CESM-DP but not in the CESM-LE. The key role of oceanic dynamics in driving the decadal variability of North Atlantic SST has been recognized by recent studies (e.g., Delworth et al. 2017; Kim et al. 2018), and initializing the model with realistic subsurface ocean conditions in the CESM-DP contributes to

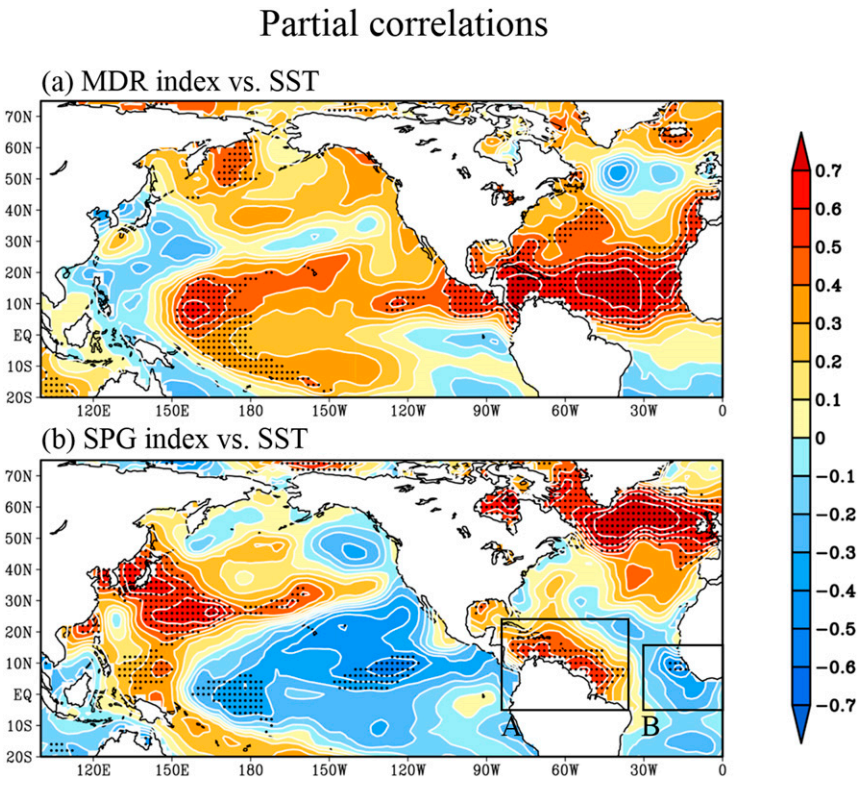

FIG. 10. Partial correlations of the observed 5-yr-mean global SST with the (a) MDR SST index and (b) SPG SST index from 1955 to 2016. Black dots indicate the regions exceeding the 95% confidence level based on the Student's *t* test. The Atlantic dipole index is defined as the averaged SST difference between region A (5°S–22°N, 35°–85°W) and region B (5°S–15°N, 0°–30°W).

the skillful predictions of the AMOC and the SPG SST. In contrast, the evolution of tropical SST is believed to be driven by radiative forcing associated with time-varying greenhouse gases and aerosols (Booth et al. 2012; Evan et al. 2008, 2009). The CESM-LE thus has skill in predicting the MDR SST even without the ocean initialization. The comparison also implies the role of external forcing in the variability of Atlantic basinwide TC frequency.

Further analysis is conducted to evaluate how the SPG SST may affect the large-scale environmental conditions. It is shown that the SPG SST can modulate VWS and TPW over the tropical Atlantic independent of the MDR SST forcing, and it plays a role in modulating the strength of the Atlantic regional Hadley circulation. In addition to being affected by the local SST, the atmospheric circulation over the tropical Atlantic is also subject to remote SST forcing from the Pacific (Li et al. 2015). Although the hybrid model does not use any SST index from the Pacific, the significant correlation between the observed SPG SST and PDO indices suggests that the remote influence from the Pacific is partly represented by the SPG SST in the hybrid model.

It is worth pointing out that this study is based on the hindcasts of one climate model (CESM). Some results, such as the relative importance of the SPG SST and MDR SST in the multiyear variability of Atlantic TC activity, may be model dependent. Additionally, the impacts of SPG SST on tropical Atlantic climate variability are largely inferred from observational analyses and the findings of previous studies. Although partial correlations and regressions are used to assess the relative impacts of the MDR and SPG SST on Atlantic TC activity and atmospheric circulation, it is challenging to clearly disentangle them using observational data alone, especially given possible nonlinear relations. The physical connection between the SPG SST and tropical Atlantic atmospheric circulation needs to be further explored by idealized climate simulations.

Acknowledgments. This work is supported by the National Oceanic and Atmospheric Administration (NOAA) Grant NA16OAR4310080. We thank Drs. Baoqiang Xiang and Ryan Sriver for the stimulating discussion. The CESM-LE outputs are available at https://www.earthsystemgrid.org/,

and the CESM-DP and FOSI outputs are available at http://www.cesm.ucar.edu/projects/community-projects/DPLE/data-sets.html.

REFERENCES

Adler, R. F., and Coauthors, 2003: The version-2 Global Precipitation Climatology Project (GPCP) monthly precipitation analysis (1979–present). *J. Hydrometeor.*, **4**, 1147–1167, https://doi.org/10.1175/1525-7541(2003)004<1147:TVGPCP>2.0.CO;2.

Bell, G. D., and M. Chelliah, 2006: Leading tropical modes associated with interannual and multidecadal fluctuations in North Atlantic hurricane activity. *J. Climate*, **19**, 590–612, https://doi.org/10.1175/JCLI3659.1.

Bellomo, K., A. C. Clement, L. N. Murphy, L. M. Polvani, and M. A. Cane, 2016: New observational evidence for a positive cloud feedback that amplifies the Atlantic Multidecadal Oscillation. *Geophys. Res. Lett.*, **43**, 9852–9859, https://doi.org/10.1002/2016GL069961.

Booth, B. B. B., N. J. Dunstone, P. R. Halloran, T. Andrews, and N. Bellouin, 2012: Aerosols implicated as a prime driver of twentieth-century North Atlantic climate variability. *Nature*, **484**, 228–232, https://doi.org/10.1038/nature10946.

Broccoli, A. J., K. A. Dahl, and R. J. Stouffer, 2006: Response of the ITCZ to Northern Hemisphere cooling. *Geophys. Res. Lett.*, **33**, L01702, https://doi.org/10.1029/2005GL024546.

Camargo, S. J., K. A. Emanuel, and A. H. Sobel, 2007: Use of a genesis potential index to diagnose ENSO effects on tropical cyclone genesis. *J. Climate*, **20**, 4819–4834, https://doi.org/10.1175/JCLI4282.1.

Cane, M. A., A. C. Clement, L. N. Murphy, and K. Bellomo, 2017: Low-pass filtering, heat flux, and Atlantic multidecadal variability. *J. Climate*, **30**, 7529–7553, https://doi.org/10.1175/JCLI-D-16-0810.1.

Caron, L.-P., C. G. Jones, and F. Doblas-Reyes, 2014: Multi-year prediction skill of Atlantic hurricane activity in CMIP5 decadal hindcasts. *Climate Dyn.*, **42**, 2675–2690, https://doi.org/10.1007/s00382-013-1773-1.

——, M. Boudreault, and C. L. Bruyère, 2015a: Changes in large-scale controls of Atlantic tropical cyclone activity with the phases of the Atlantic Multidecadal Oscillation. *Climate Dyn.*, **44**, 1801–1821, https://doi.org/10.1007/s00382-014-2186-5.

——, L. Hermanson, and F. J. Doblas-Reyes, 2015b: Multiannual forecasts of Atlantic U.S. tropical cyclone wind damage potential. *Geophys. Res. Lett.*, **42**, 2417–2425, https://doi.org/10.1002/2015GL063303.

——, ——, A. Dobbin, J. Imbers, L. Lledó, and G. A. Vecchi, 2018: How skillful are the multiannual forecasts of Atlantic hurricane activity? *Bull. Amer. Meteor. Soc.*, **99**, 403–413, https://doi.org/10.1175/BAMS-D-17-0025.1.

Chafik, L., S. Häkkinen, M. H. England, J. A. Carton, S. Nigam, A. Ruiz-Barradas, A. Hannachi, and L. Miller, 2016: Global linkages originating from decadal oceanic variability in the subpolar North Atlantic. *Geophys. Res. Lett.*, **43**, 10 909–10 919, https://doi.org/10.1002/2016GL071134.

Chang, C.-C., and Z. Wang, 2018: Relative impacts of local and remote forcing on tropical cyclone frequency in numerical model simulations. *Geophys. Res. Lett.*, **45**, 7843–7850, https://doi.org/10.1029/2018GL078606.

Chelton, D. B., 1984. Commentary: Short-term climatic variability in the Northeast Pacific Ocean. *The Influence of Ocean Conditions on the Production of Salmonids in the North Pacific*, W. Pearcy, Ed., Oregon State University Press, 87–99.

Chen, J.-H., and S.-J. Lin, 2011: The remarkable predictability of inter-annual variability of Atlantic hurricanes during the past decade. *Geophys. Res. Lett.*, **38**, L11804, https://doi.org/10.1029/2011GL047629.

——, and ——, 2013: Seasonal predictions of tropical cyclones using a 25-km-resolution general circulation model. *J. Climate*, **26**, 380–398, https://doi.org/10.1175/JCLI-D-12-00061.1.

Chiang, J. C. H., 2002: Deconstructing Atlantic Intertropical Convergence Zone variability: Influence of the local cross-equatorial sea surface temperature gradient and remote forcing from the eastern equatorial Pacific. *J. Geophys. Res.*, **107**, 4004, https://doi.org/10.1029/2000JD000307.

——, and C. M. Bitz, 2005: Influence of high latitude ice cover on the marine Intertropical Convergence Zone. *Climate Dyn.*, **25**, 477–496, https://doi.org/10.1007/s00382-005-0040-5.

——, M. Biasutti, and D. S. Battisti, 2003: Sensitivity of the Atlantic Intertropical Convergence Zone to Last Glacial Maximum boundary conditions. *Paleoceanography*, **18**, 1094, https://doi.org/10.1029/2003PA000916.

Clement, A., K. Bellomo, L. N. Murphy, M. A. Cane, T. Mauritsen, G. Radel, and B. Stevens, 2015: The Atlantic Multidecadal Oscillation without a role for ocean circulation. *Science*, **350**, 320–324, https://doi.org/10.1126/science.aab3980.

Czaja, A., and J. Marshall, 2001: Observations of atmosphere–ocean coupling in the North Atlantic. *Quart. J. Roy. Meteor. Soc.*, **127**, 1893–1916, https://doi.org/10.1002/qj.49712757603.

Danabasoglu, G., S. C. Bates, B. P. Briegleb, S. R. Jayne, M. Jochum, W. G. Large, S. Peacock, and S. G. Yeager, 2012: The CCSM4 ocean component. *J. Climate*, **25**, 1361–1389, https://doi.org/10.1175/JCLI-D-11-00091.1.

Davis, C. E., J. E. Hyde, S. I. Bangdiwala, and J. J. Nelson, 1986: An example of dependencies among variables in a conditional logistic regression. *Modern Statistical Methods in Chronic Disease Epidemiology*, S. H. Moolgavkar and R. L. Prentice, Eds., Wiley, 140–147.

Delworth, T. L., F. Zeng, L. Zhang, R. Zhang, G. A. Vecchi, and X. Yang, 2017: The central role of ocean dynamics in connecting the North Atlantic Oscillation to the extratropical component of the Atlantic multidecadal oscillation. *J. Climate*, **30**, 3789–3805, https://doi.org/10.1175/JCLI-D-16-0358.1.

Diatta, S., and A. H. Fink, 2014: Statistical relationship between remote climate indices and West African monsoon variability. *Int. J. Climatol.*, **34**, 3348–3367, https://doi.org/10.1002/joc.3912.

Dong, B.-W., and R. T. Sutton, 2002: Adjustment of the coupled ocean–atmosphere system to a sudden change in the thermohaline circulation. *Geophys. Res. Lett.*, **29**, 1728, https://doi.org/10.1029/2002GL015229.

Dunstone, N. J., D. M. Smith, and R. Eade, 2011: Multi-year predictability of the tropical Atlantic atmosphere driven by the high latitude North Atlantic Ocean. *Geophys. Res. Lett.*, **38**, L14701, https://doi.org/10.1029/2011GL047949.

Evan, A. T., and Coauthors, 2008: Ocean temperature forcing by aerosols across the Atlantic tropical cyclone development region. *Geochem. Geophys. Geosyst.*, **9**, Q05V04, https://doi.org/10.1029/2007GC001774.

——, D. J. Vimont, A. K. Heidinger, J. P. Kossin, and R. Bennartz, 2009: The role of aerosols in the evolution of tropical North Atlantic Ocean temperature anomalies. *Science*, **324**, 778–781, https://doi.org/10.1126/science.1167404.

Gall, R., J. Franklin, F. Marks, E. N. Rappaport, and F. Toepfer, 2013: The Hurricane Forecast Improvement Project. *Bull.*

Amer. Meteor. Soc., **94**, 329–343, https://doi.org/10.1175/BAMS-D-12-00071.1.

Goldenberg, S. B., and L. J. Shapiro, 1996: Physical mechanisms for the association of El Niño and West African rainfall with Atlantic major hurricane activity. *J. Climate*, **9**, 1169–1187, https://doi.org/10.1175/1520-0442(1996)009<1169:PMFTAO>2.0.CO;2.

——, C. W. Landsea, A. M. Mestas-Nuñez, and W. M. Gray, 2001: The recent increase in Atlantic hurricane activity: Causes and implications. *Science*, **293**, 474–479, https://doi.org/10.1126/science.1060040.

Gualdi, S., E. Scoccimarro, and A. Navarra, 2008: Changes in tropical cyclone activity due to global warming: Results from a high-resolution coupled general circulation model. *J. Climate*, **21**, 5204–5228, https://doi.org/10.1175/2008JCLI1921.1.

Huang, B., and Coauthors, 2017: Extended Reconstructed Sea Surface Temperature, version 5 (ERSSTv5): Upgrades, validations, and intercomparisons. *J. Climate*, **30**, 8179–8205, https://doi.org/10.1175/JCLI-D-16-0836.1.

Hurrell, J. W., and Coauthors, 2013: The Community Earth System Model: A framework for collaborative research. *Bull. Amer. Meteor. Soc.*, **94**, 1339–1360, https://doi.org/10.1175/BAMS-D-12-00121.1.

Kalnay, E., and Coauthors, 1996: The NCEP/NCAR 40-Year Reanalysis Project. *Bull. Amer. Meteor. Soc.*, **77**, 437–471, https://doi.org/10.1175/1520-0477(1996)077<0437:TNYRP>2.0.CO;2.

Kang, S. M., I. M. Held, D. M. W. Frierson, and M. Zhao, 2008: The response of the ITCZ to extratropical thermal forcing: Idealized slab-ocean experiments with a GCM. *J. Climate*, **21**, 3521–3532, https://doi.org/10.1175/2007JCLI2146.1.

——, D. M. W. Frierson, and I. M. Held, 2009: The tropical response to extratropical thermal forcing in an idealized GCM: The importance of radiative feedbacks and convective parameterization. *J. Atmos. Sci.*, **66**, 2812–2827, https://doi.org/10.1175/2009JAS2924.1.

Kay, J. E., and Coauthors, 2015: The Community Earth System Model (CESM) large ensemble project: A community resource for studying climate change in the presence of internal climate variability. *Bull. Amer. Meteor. Soc.*, **96**, 1333–1349, https://doi.org/10.1175/BAMS-D-13-00255.1.

Kim, W. M., S. G. Yeager, and G. Danabasoglu, 2018: Key role of internal ocean dynamics in Atlantic multidecadal variability during the last half century. *Geophys. Res. Lett.*, **45**, 13 449–13 457, https://doi.org/10.1029/2018GL080474.

Klotzbach, P. J., 2007: Revised prediction of seasonal Atlantic basin tropical cyclone activity from 1 August. *Wea. Forecasting*, **22**, 937–949, https://doi.org/10.1175/WAF1045.1.

Knight, J. R., C. K. Folland, and A. A. Scaife, 2006: Climate impacts of the Atlantic Multidecadal Oscillation. *Geophys. Res. Lett.*, **33**, L17706, https://doi.org/10.1029/2006GL026242.

Landsea, C. W., and J. L. Franklin, 2013: Atlantic hurricane database uncertainty and presentation of a new database format. *Mon. Wea. Rev.*, **141**, 3576–3592, https://doi.org/10.1175/MWR-D-12-00254.1.

Latif, M., N. Keenlyside, and J. Bader, 2007: Tropical sea surface temperature, vertical wind shear, and hurricane development. *Geophys. Res. Lett.*, **34**, L01710, https://doi.org/10.1029/2006GL027969.

Li, W., L. Li, and Y. Deng, 2015: Impact of the Interdecadal Pacific Oscillation on tropical cyclone activity in the North Atlantic and eastern North Pacific. *Sci. Rep.*, **5**, 12358, https://doi.org/10.1038/srep12358.

Manganello, J. V., and Coauthors, 2012: Tropical cyclone climatology in a 10-km global atmospheric GCM: Toward weather-resolving climate modeling. *J. Climate*, **25**, 3867–3893, https://doi.org/10.1175/JCLI-D-11-00346.1.

——, and Coauthors, 2016: Seasonal forecasts of tropical cyclone activity in a high-atmospheric-resolution coupled prediction system. *J. Climate*, **29**, 1179–1200, https://doi.org/10.1175/JCLI-D-15-0531.1.

Martin, E. R., and C. D. Thorncroft, 2014: The impact of the AMO on the West African monsoon annual cycle. *Quart. J. Roy. Meteor. Soc.*, **140**, 31–46, https://doi.org/10.1002/qj.2107.

McCullagh, P., and J. A. Nelder, 1989: *Generalized Linear Models*. 2nd ed. Chapman and Hall/CRC, 532 pp.

McGregor, S., A. Timmermann, M. F. Stuecker, M. H. England, M. Merrifield, F.-F. Jin, and Y. Chikamoto, 2014: Recent Walker circulation strengthening and Pacific cooling amplified by Atlantic warming. *Nat. Climate Change*, **4**, 888–892, https://doi.org/10.1038/nclimate2330.

Mei, W., Y. Kamae, S.-P. Xie, and K. Yoshida, 2019: Variability and predictability of North Atlantic hurricane frequency in a large ensemble of high-resolution atmospheric simulations. *J. Climate*, **32**, 3153–3167, https://doi.org/10.1175/JCLI-D-18-0554.1.

Murakami, H., and Coauthors, 2015: Simulation and prediction of category 4 and 5 hurricanes in the high-resolution GFDL HiFLOR coupled climate model. *J. Climate*, **28**, 9058–9079, https://doi.org/10.1175/JCLI-D-15-0216.1.

Okumura, Y. M., C. Deser, A. Hu, A. Timmermann, and S. Xie, 2009: North Pacific climate response to freshwater forcing in the subarctic North Atlantic: Oceanic and atmospheric pathways. *J. Climate*, **22**, 1424–1445, https://doi.org/10.1175/2008JCLI2511.1.

Otterå, O. H., M. Bentsen, H. Drange, and L. Suo, 2010: External forcing as a metronome for Atlantic multidecadal variability. *Nat. Geosci.*, **3**, 688–694, https://doi.org/10.1038/ngeo955.

Otto-Bliesner, B. L., and Coauthors, 2016: Climate variability and change since 850 CE: An ensemble approach with the Community Earth System Model. *Bull. Amer. Meteor. Soc.*, **97**, 735–754, https://doi.org/10.1175/BAMS-D-14-00233.1.

Ramsay, H. A., and A. H. Sobel, 2011: Effects of relative and absolute sea surface temperature on tropical cyclone potential intensity using a single-column model. *J. Climate*, **24**, 183–193, https://doi.org/10.1175/2010JCLI3690.1.

Raymond, D. J., 1995: Regulation of moist convection over the West Pacific warm pool. *J. Atmos. Sci.*, **52**, 3945–3959, https://doi.org/10.1175/1520-0469(1995)052<3945:ROMCOT>2.0.CO;2.

Ruprich-Robert, Y., R. Msadek, F. Castruccio, S. Yeager, T. Delworth, and G. Danabasoglu, 2017: Assessing the climate impacts of the observed Atlantic multidecadal variability using the GFDL CM2.1 and NCAR CESM1 global coupled models. *J. Climate*, **30**, 2785–2810, https://doi.org/10.1175/JCLI-D-16-0127.1.

Smith, D. M., R. Eade, N. J. Dunstone, D. Fereday, J. M. Murphy, H. Pohlmann, and A. A. Scaife, 2010: Skilful multi-year predictions of Atlantic hurricane frequency. *Nat. Geosci.*, **3**, 846–849, https://doi.org/10.1038/ngeo1004.

Sobel, A. H., and C. S. Bretherton, 2000: Modeling tropical precipitation in a single column. *J. Climate*, **13**, 4378–4392, https://doi.org/10.1175/1520-0442(2000)013<4378:MTPIAS>2.0.CO;2.

——, I. M. Held, and C. S. Bretherton, 2002: The ENSO signal in tropical tropospheric temperature. *J. Climate*, **15**, 2702–2706, https://doi.org/10.1175/1520-0442(2002)015<2702:TESITT>2.0.CO;2.

Sohn, B. J., S.-W. Yeh, J. Schmetz, and H.-J. Song, 2013: Observational evidences of Walker circulation change over the last 30 years contrasting with GCM results. *Climate Dyn.*, **40**, 1721–1732, https://doi.org/10.1007/s00382-012-1484-z.

Sugi, M., H. Murakami, and J. Yoshimura, 2012: On the mechanism of tropical cyclone frequency changes due to global warming. *J. Meteor. Soc. Japan*, **90A**, 397–408, https://doi.org/10.2151/jmsj.2012-A24.

Sutton, R. T., 2005: Atlantic Ocean forcing of North American and European summer climate. *Science*, **309**, 115–118, https://doi.org/10.1126/science.1109496.

——, and D. L. R. Hodson, 2007: Climate response to basin-scale warming and cooling of the North Atlantic Ocean. *J. Climate*, **20**, 891–907, https://doi.org/10.1175/JCLI4038.1.

Swanson, K. L., 2008: Nonlocality of Atlantic tropical cyclone intensities. *Geochem. Geophys. Geosyst.*, **9**, Q04V01, https://doi.org/10.1029/2007GC001844.

Vecchi, G. A., and B. J. Soden, 2007: Effect of remote sea surface temperature change on tropical cyclone potential intensity. *Nature*, **450**, 1066–1070, https://doi.org/10.1038/nature06423.

——, M. Zhao, H. Wang, G. Villarini, A. Rosati, A. Kumar, I. M. Held, and R. Gudgel, 2011: Statistical–dynamical predictions of seasonal North Atlantic hurricane activity. *Mon. Wea. Rev.*, **139**, 1070–1082, https://doi.org/10.1175/2010MWR3499.1.

——, and Coauthors, 2013: Multiyear predictions of North Atlantic hurricane frequency: Promise and limitations. *J. Climate*, **26**, 5337–5357, https://doi.org/10.1175/JCLI-D-12-00464.1.

——, and Coauthors, 2014: On the seasonal forecasting of regional tropical cyclone activity. *J. Climate*, **27**, 7994–8016, https://doi.org/10.1175/JCLI-D-14-00158.1.

Villarini, G., G. A. Vecchi, and J. A. Smith, 2012: U.S. landfalling and North Atlantic hurricanes: Statistical modeling of their frequencies and ratios. *Mon. Wea. Rev.*, **140**, 44–65, https://doi.org/10.1175/MWR-D-11-00063.1.

Vimont, D. J., and J. P. Kossin, 2007: The Atlantic meridional mode and hurricane activity. *Geophys. Res. Lett.*, **34**, L07709, https://doi.org/10.1029/2007GL029683.

Walsh, K., S. Lavender, H. Murakami, E. Scoccimarro, L.-P. Caron, and M. Ghantous, 2010: The tropical cyclone climate model intercomparison project. *Hurricanes and Climate Change*, J. B. Elsner et al., Eds., Springer, 1–24.

Wentz, F. J., and M. Schabel, 2000: Precise climate monitoring using complementary satellite data sets. *Nature*, **403**, 414–416, https://doi.org/10.1038/35000184.

Wilks, D. S., 2006: *Statistical Methods in the Atmospheric Sciences*. 2nd ed. Academic Press, 627 pp.

Yeager, S., and G. Danabasoglu, 2014: The origins of late-twentieth-century variations in the large-scale North Atlantic circulation. *J. Climate*, **27**, 3222–3247, https://doi.org/10.1175/JCLI-D-13-00125.1.

——, A. Karspeck, G. Danabasoglu, J. Tribbia, and H. Teng, 2012: A decadal prediction case study: Late twentieth-century North Atlantic Ocean heat content. *J. Climate*, **25**, 5173–5189, https://doi.org/10.1175/JCLI-D-11-00595.1.

——, and Coauthors, 2018: Predicting near-term changes in the Earth system: A large ensemble of initialized decadal prediction simulations using the Community Earth System Model. *Bull. Amer. Meteor. Soc.*, **99**, 1867–1886, https://doi.org/10.1175/BAMS-D-17-0098.1.

Yu, J.-Y., P. Kao, H. Paek, H.-H. Hsu, C. Hung, M.-M. Lu, and S.-I. An, 2015: Linking emergence of the central Pacific El Niño to the Atlantic multidecadal oscillation. *J. Climate*, **28**, 651–662, https://doi.org/10.1175/JCLI-D-14-00347.1.

Yuan, T., L. Oreopoulos, M. Zelinka, H. Yu, J. R. Norris, M. Chin, S. Platnick, and K. Meyer, 2016: Positive low cloud and dust feedbacks amplify tropical North Atlantic multidecadal oscillation. *Geophys. Res. Lett.*, **43**, 1349–1356, https://doi.org/10.1002/2016GL067679.

Zeng, N., J. D. Neelin, and C. Chou, 2000: A quasi-equilibrium tropical circulation model—Implementation and simulation. *J. Atmos. Sci.*, **57**, 1767–1769, https://doi.org/10.1175/1520-0469(2000)057<1767:AQETCM>2.0.CO;2.

Zhang, G., and Z. Wang, 2013: Interannual variability of the Atlantic Hadley circulation in boreal summer and its impacts on tropical cyclone activity. *J. Climate*, **26**, 8529–8544, https://doi.org/10.1175/JCLI-D-12-00802.1.

——, and ——, 2019: North Atlantic Rossby wave breaking during the hurricane season: Association with tropical and extratropical variability. *J. Climate*, **32**, 3777–3801, https://doi.org/10.1175/JCLI-D-18-0299.1.

——, ——, T. J. Dunkerton, M. S. Peng, and G. Magnusdottir, 2016: Extratropical impacts on Atlantic tropical cyclone activity. *J. Atmos. Sci.*, **73**, 1401–1418, https://doi.org/10.1175/JAS-D-15-0154.1.

——, ——, M. S. Peng, and G. Magnusdottir, 2017: Characteristics and impacts of extratropical Rossby wave breaking during the Atlantic hurricane season. *J. Climate*, **30**, 2363–2379, https://doi.org/10.1175/JCLI-D-16-0425.1.

——, T. Knutson, and S. Garner, 2019: Impacts of extratropical weather perturbations on tropical cyclone activity: Idealized sensitivity experiments with a regional atmospheric model. *Geophys. Res. Lett.*, **46**, 14 052–14 062, https://doi.org/10.1029/2019GL085398.

Zhang, L., and C. Zhao, 2015: Processes and mechanisms for the model SST biases in the North Atlantic and North Pacific: A link with the Atlantic meridional overturning circulation. *J. Adv. Model. Earth Syst.*, **7**, 739–758, https://doi.org/10.1002/2014MS000415.

Zhang, R., and T. L. Delworth, 2005: Simulated tropical response to a substantial weakening of the Atlantic thermohaline circulation. *J. Climate*, **18**, 1853–1860, https://doi.org/10.1175/JCLI3460.1.

——, and ——, 2006: Impact of Atlantic multidecadal oscillations on India/Sahel rainfall and Atlantic hurricanes. *Geophys. Res. Lett.*, **33**, L17712, https://doi.org/10.1029/2006GL026267.

——, and ——, 2007: Impact of the Atlantic Multidecadal Oscillation on North Pacific climate variability. *Geophys. Res. Lett.*, **34**, L23708, https://doi.org/10.1029/2007GL031601.

——, and Coauthors, 2019: A review of the role of the Atlantic meridional overturning circulation in Atlantic multidecadal variability and associated climate impacts. *Rev. Geophys.*, **57**, 316–375, https://doi.org/10.1029/2019RG000644.

Zhang, Y., J. M. Wallace, and D. S. Battisti, 1997: ENSO-like interdecadal variability: 1900–93. *J. Climate*, **10**, 1004–1020, https://doi.org/10.1175/1520-0442(1997)010<1004:ELIV>2.0.CO;2.

Zhao, M., I. M. Held, and G. A. Vecchi, 2010: Retrospective forecasts of the hurricane season using a global atmospheric model assuming persistence of SST anomalies. *Mon. Wea. Rev.*, **138**, 3858–3868, https://doi.org/10.1175/2010MWR3366.1.